ANALYTICAL MODEL OF INVERSION LAYER QUANTIZATION EFFECTS IN HEAVILY DOPED N-CHANNEL MOSFETS

A Thesis submitted to the Electrical and Electronic
Engineering Department of BUET, Dhaka,
in partial fulfilment of the
requirements for the degree of
Master of Science in Engineering
(Electrical and Electronic)

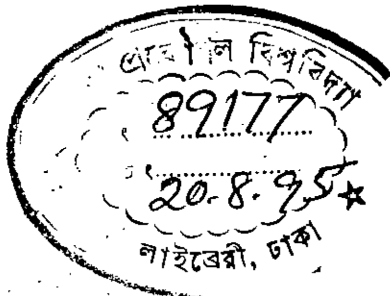

ABDUL MUBIN AHMED

AUGUST 1995

The thesis 'Analytical Model of Inversion Layer Quantization Effects in Heavily Doped N-channel MOSFETs' submitted by Abdul Mubin Ahmed, Roll No.921357P, session 1990-91-92 to the Electrical and Electronic Engineering Department of BUET has been accepted as satisfactory for partial fulfilment of the requirements for the degree of Master of Science in Engineering (Electrical and Electronic).

Board of Examiners

1. Dr. M.M. Shahidul Hassan
   Associate Professor
   EEE Department
   BUET., Dhaka-1000

   Chairman ______ 3/8/95
   (Supervisor)

2. Dr. A.B.M.Siddique Hossain
   Professor & Head
   EEE Department
   BUET., Dhaka-1000

   Member ______ 03/08/95
   (Ex-officio)

3. Dr. Md. Rezwan Khan
   Associate Professor
   EEE Department
   BUET., Dhaka-1000

   Member ______ 3.8.95

4. Dr. Gias Uddin Ahmad
   Professor
   Department of Physics
   BUET., Dhaka-1000

   Member ______ 3-8-95
   (External)

DECLARATION

I hereby declare that this work has been done by me and it has not been submitted elsewhere for the award of any degree or diploma.

Countersigned

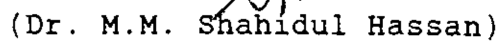

(Dr. M.M. Shahidul Hassan)
Supervisor

(Abdul Mubin Ahmed)

CONTENTS

ACKNOWLEDGEMENTS iv

ABSTRACT v

LIST OF FIGURES vi

1. INTRODUCTION 1

1.1 Threshold voltage of MOSFETs.................... 1
1.2 Quantum effects on threshold voltage............. 9
1.3 Review of past and present works on quantization effects on threshold voltage........ 12
1.4 Objective of this work........................... 13
1.5 Summary of the thesis............................ 14

2. MATHEMATICAL ANALYSIS FOR THRESHOLD VOLTAGE OF MOSFETS UNDER INVERSION CONSIDERING QUANTIZATION EFFECTS 16

2.1 Introduction..................................... 16

2.2 WKB approximation.................................. 18
2.2.1 Introduction................................ 18
2.2.2 The one-dimensional Schrödinger wave equation................................ 18
2.2.3 Approximate solutions..................... 20
2.2.4 Solution near a turning point............. 22
2.2.5 Linear turning point...................... 23
2.2.6 Connection at a turning point............. 25
2.2.7 Asymptotic connection formulas............ 27
2.3 Eigen energy of a triangular potential well...... 28
2.4 Average separation of minority carriers.......... 35
2.5 Quantum threshold voltage........................ 36
2.6 Summary.. 41

3. RESULTS BASED ON ANALYTICAL SOLUTION 43

3.1 Introduction..................................... 43
3.2 Computational method in studying MOS device....... 43
3.3 Results and discussions.......................... 44
3.3.1 Energy level shift.......................... 44
3.3.2 Inversion layer concentration.............. 47
3.3.3 Depletion layer concentration.............. 49
3.3.4 The average penetration of the inversion layer charge density from the surface..... 49
3.3.5 Threshold voltage shift..................... 53
3.4 Summary.. 55

4. CONCLUSIONS 58

4.1 Conclusions.................................... 58

4.2 Suggestions for future work...................... 59

REFERENCES 60

ACKNOWLEDGEMENTS

The author would like to express his sincere gratitude to Dr. M.M.Shahidul Hassan, Associate Professor of the Department of Electrical and Electronic Engineering, BUET, for his endless patience, friendly supervision and specially for the encouragement and support that he provided at the vital phases of the work.

The author wishes to express his thanks and regards to Dr. A.B.M. Siddique Hossain, Professor and Head of the Department of Electrical and Electronic Engineering, BUET, for his support during the work.

Thanks to all colleagues and friends for their support. The author is truly greatful to his parents, sister and wife for their full support and cooperation.

ABSTRACT

MOSFETs are extensively used in IC fabrications. Improvement of the VLSI technology has resulted in device dimensions of the order of fractions of a micron. With increased substrate doping levels and reduced gate oxide thicknesses the classical treatment of MOSFETs is no longer accurate. If the substrate is heavily doped then the inversion layer thickness falls below the classical critical width and under that situation the quantization effects cannot be neglected. The effects of quantization can be most accurately modeled by numerically solving Schrödinger's and Poisson's equations self-consistently. But this approach involves much computational time. It is important to develop a computer efficient method that can derive a result that approximates the quantum mechanical calculation results. In this thesis WKB approximate method is used to determine the eigen energy of the inversion layer potential well. The average penetration of the inversion layer charges in the potential well from the semiconductor-insulator interface is determined using the results of the WKB method. The surface potential at the semiconductor-insulator interface is then related to the threshold voltage by using the calculated eigen energy and the average penetration of the inversion layer charges from the semiconductor-insulator interface. The derived relations are used to develop a computer efficient analytical model to study the quantum mechanical effects in various parameters of MOSFETs including threshold voltage. The threshold voltage is found to be larger than the classical value if quantization effects are considered. Also quantization effects are found to become prominent for higher substrate doping levels and thinner gate oxide thicknesses.

LIST OF FIGURES

1.1 Substrate band diagram.............................. 3
1.2 Substrate band diagram at higher gate voltage........ 5
1.3 Substrate band diagram at threshold condition........ 6
1.4 The schematic cross-section of an n-channel MOSFET... 9
1.5 Quantum-mechanical effects on inversion layer charge.. 11
2.1 Linear turning point................................ 24
2.2 Electrostatic potential well........................ 30
2.3 Potential trough.................................... 31
2.4 Band bending due to depletion charges............... 39
3.1 Effect of surface electric field on the lowest energy subband................................ 45
3.2 Lowest energy subband vs. inversion layer charge.... 46
3.3 Effect of surface potential on inversion layer charge....................................... 48
3.4 Effect of surface potential on depletion charges.... 50
3.5 Inversion and depletion charges vs. surface potential.. 51
3.6 Effect of surface electric field on average penetration of inversion charges from the Si/SiO_2 interface.. 52
3.7 Effect of channel doping on the difference between quantum and classical threshold voltage..... 54

CHAPTER 1

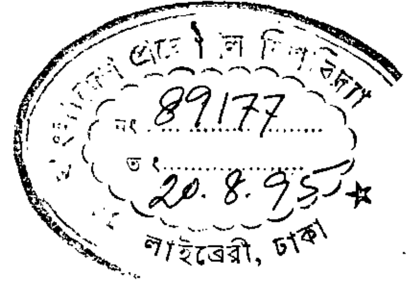

INTRODUCTION

1.1 Threshold voltage of MOSFETs

An important parameter in MOS transistors (Fig.1.1) is the threshold voltage V_T, which is the minimum gate voltage required to induce the channel. For an n-channel enhancement type MOSFET, the positive gate voltage must be greater than some value V_T before conducting channel is induced. Similarly a p-channel MOSFET requires a gate voltage more negative than some value V_T to induce the required holes in the channel.

The electron and hole concentrations at equilibrium can be expressed as follows [1]:

$$n = n_i \, e^{\frac{q}{kT}(\psi-\phi_F)} \qquad (1.1)$$

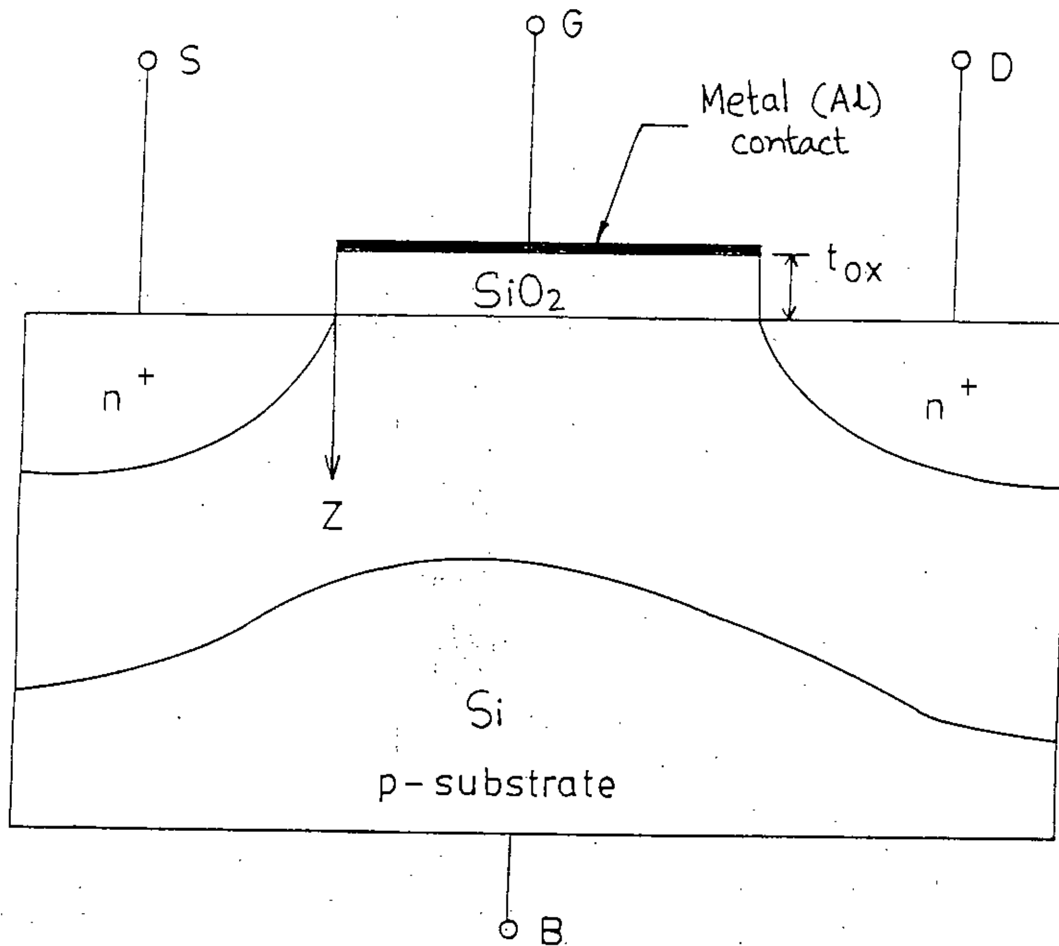

Fig. 1.1 The schematic cross section of an n-channel MOSFET.

and

$$p = n_i \, e^{\frac{q}{kT}(\phi_F - \psi)} \qquad (1.2)$$

where, n_i is the intrinsic carrier concentration, k is Boltzmann's constant, T is the absolute temperature, ψ is the potential of the intrinsic energy level, and ϕ_F is the Fermi potential. Taking the intrinsic level potential in the bulk region of the substrate as zero, the electron concentration can be written as,

$$n = N_A \, e^{\left(\frac{q}{kT}(\psi - 2\phi_F)\right)} \qquad (1.3)$$

where N_A is the doping density of the substrate. The potential ψ is the potential anywhere in the semiconductor, measured from the bulk zero reference (Fig.1.2). At the surface it is called the surface potential ψ_S, and it is the total voltage drop across the semiconductor, measured from the surface to the bulk reference.

Positive gate voltage produces an electric field which bends the energy bands downward. For small positive gate voltage majority carriers i.e., holes are depleted from the vicinity of the oxide-silicon surface, establishing a space-

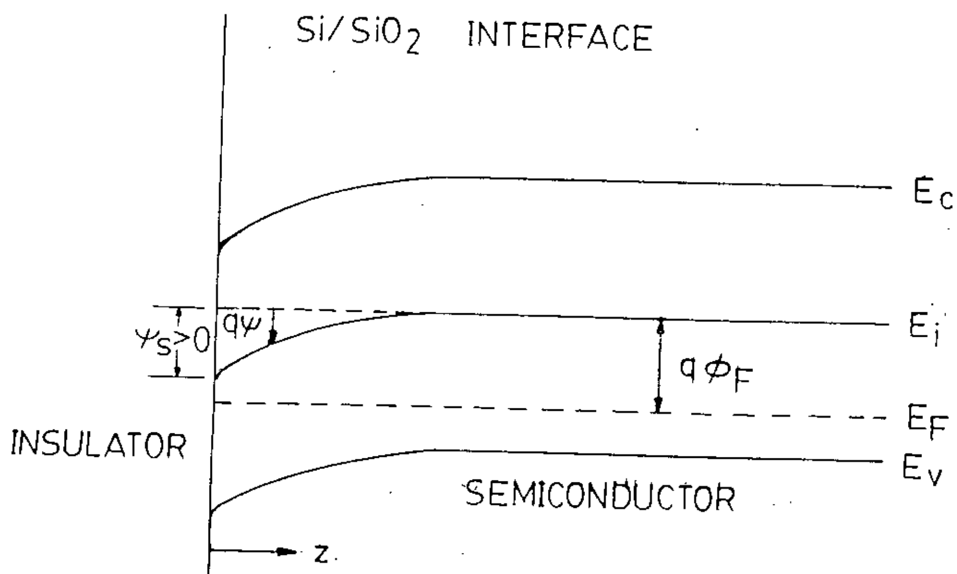

Fig. 1.2 Substrate band diagram.

charge region consisting of stationary acceptor ions. If we continue to increase the positive voltage, the bands at the semiconductor surface bend down more strongly (Fig.1.3(a)). A sufficiently large gate voltage can bend E_i below E_F and an inversion layer is formed (Fig.1.3(b)). This inversion layer near the semiconductor surface has conduction properties typical of n-type material. The generally accepted definition of strong inversion is one where the surface concentration of minority carriers is equal in magnitude to the bulk concentration of majority carriers. From the band diagram of (Fig.1.4) this means that the surface potential is as much below as the bulk potential is above the Fermi level. In other words;

$$\Psi_s = 2\Phi_F = 2\frac{kT}{q}\ln(\frac{N_A}{n_i}) \tag{1.4}$$

and

$$n_s = N_A \tag{1.5}$$

This is known as the condition of the onset of strong inversion and will be used here to specify the threshold voltage V_T in the classical treatment of MOSFETs, which follows Tsividis' treatment [2]. Threshold voltage is the critical

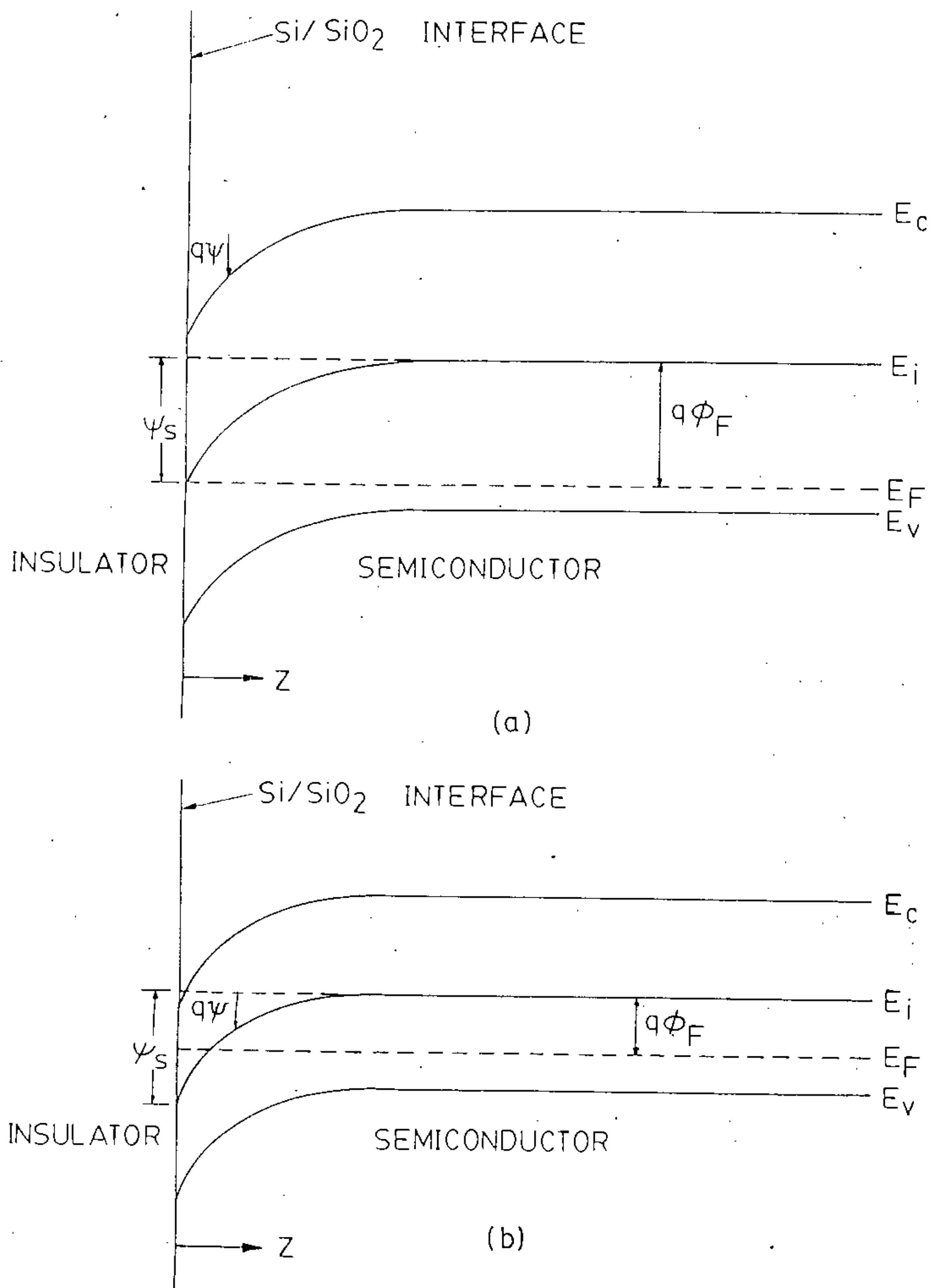

Fig. 1.3 Substrate band diagram at higher gate voltage. (a) depletion (b) inversion.

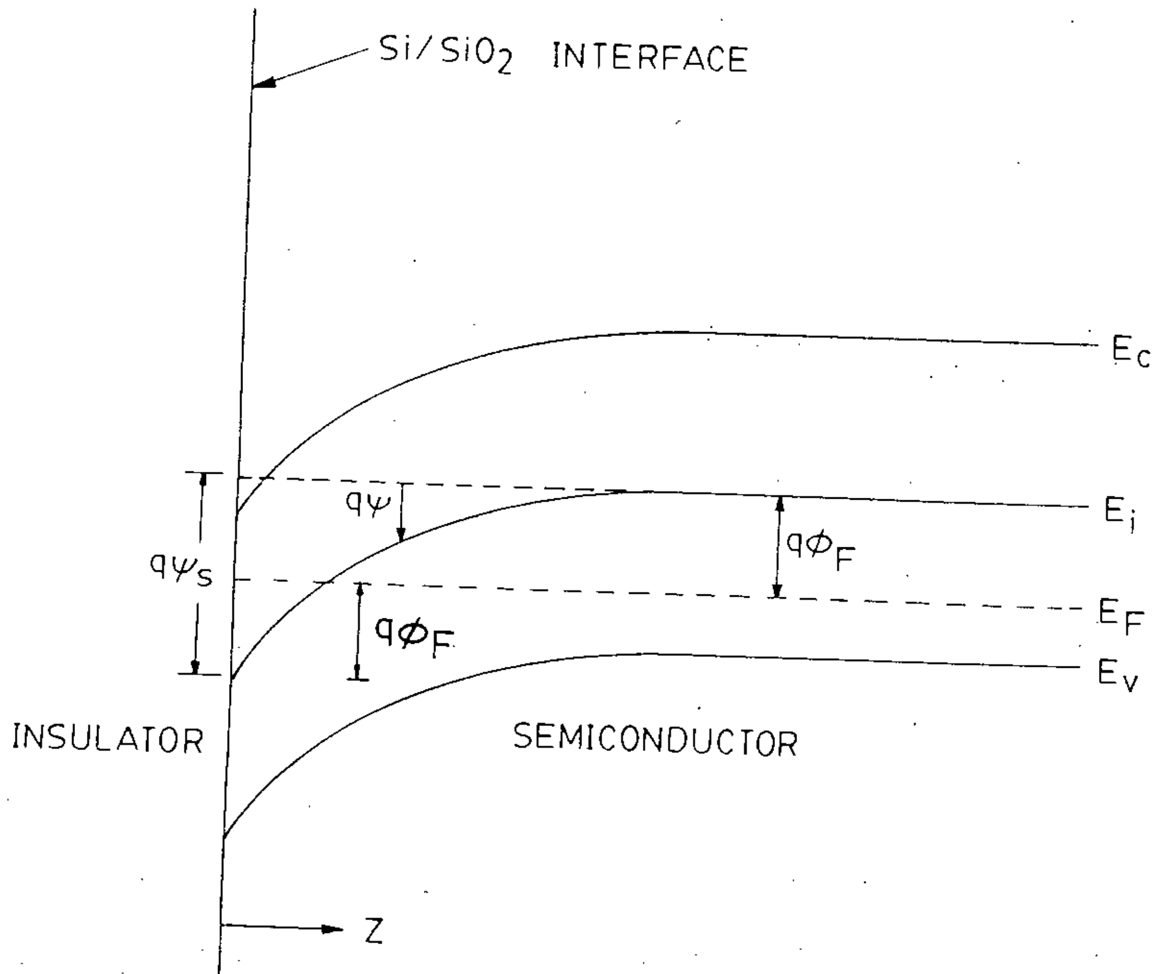

Fig. 1.4 Substrate band diagram at threshold condion.

voltage at which the inversion layer is formed to a significant extent, giving rise to rapid increase of the inversion layer charge for higher gate voltages. In other words, the threshold voltage specifies the gate voltage at strong inversion. Once strong inversion occurs, the depletion-layer width reaches a maximum. The maximum depletion width is given by [2]

$$Z_{dm} = \sqrt{\frac{2\epsilon_s \psi_s}{qN_A}} \tag{1.6}$$

The depletion charge at the classical threshold condition is given as

$$N_{depl} = N_A Z_{dm} \tag{1.7}$$

For charge neutrality of the system it is required that

$$Q_s = Q_n + qN_A Z_d \tag{1.8}$$

where, Q_s is the total charges per unit area in the semiconductor, Q_n is the electrons per unit area in the inversion region, $qN_A Z_d$ is the ionized acceptors per unit area in the space-charge region with space-charge width Z_d. Threshold voltage must support the total charges per unit area

in the semiconductor, Q_s, and at the same time introduce a band bending at the surface to reach the strong inversion potential $\psi_s = 2\phi_F$. Hence V_T is given as

$$V_T \equiv -\frac{Q_S}{C_{ox}} + \psi_S$$

$$= -\frac{Q_S}{C_{ox}} + 2\phi_F \qquad (1.9)$$

where, $C_{ox} = \epsilon_{ox}/t_{ox}$ (Fig.1.1), the capacitance per unit area of the oxide layer. Because at the onset of strong inversion, $Q_s \approx qN_A Z_{dm}$, since $Q_B >> Q_n$, the classical threshold voltage is given by

$$V_T \approx \frac{\sqrt{2\epsilon_s q N_A (2\phi_F)}}{C_{ox}} + 2\phi_F \qquad (1.10)$$

1.2 Quantum effects on threshold voltage

The effects of quantization on MOSFET have been known for decades, but only recently has it become important and necessary to physically account for these effects in MOS devices at room temperature. The combination of higher doping

levels and thinner gate oxides increases the electric field at the Si/SiO_2 interface to a level such that the energy-band bending at the Si/SiO_2 interface under inversion condition is very steep. The confinement of the carriers in this potential well leads to a two-dimensional electron gas (2DEG) system. As a result, the bulk conduction energy band is split into discrete subbands in the inversion layer, with the lowest subband shifted substantially above the conduction band minimum (Fig.1.5). The assumption of a 3-D continuum of states in a particular band, implicit in the classical treatment of inversion layer carriers, is then no longer appropriate. Therefore, in order to accurately simulate the inversion carriers in heavily doped MOS devices, models that incorporate the two-dimensional quantum nature of the carriers are necessary. The splitting of the energy band into discrete subbands has the effect of decreasing the inversion layer charge density for a given gate voltage, shifting the spatial distribution of charge in the inversion layer away from the interface and increasing the threshold voltage when compared to the classical predictions that do not include these quantum mechanical effects.

The inclusion of the various subbands in the calculation

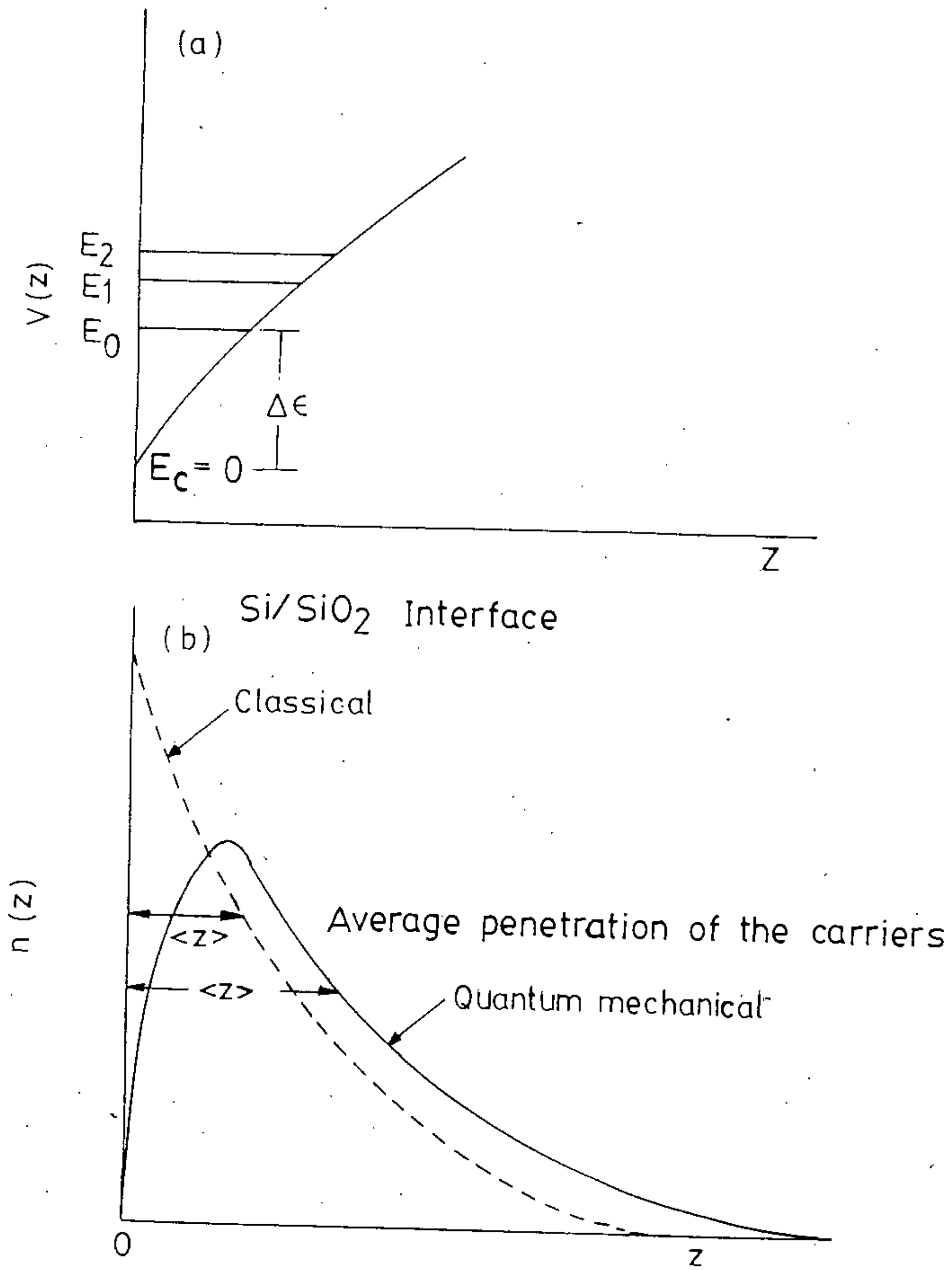

Fig. 1.5 Quantum mechanical effects on inversion layer charge.
(a) Energy layer split
(b) Spatial distribution of carriers.

of the electrical properties is hardly ever necessary for lower doping levels, because the splitting of the energy levels is usually small compared to the thermal voltage kT/q. Many of these subbands are then occupied and a quantum description of the MOS device resembles the conventional one. However, at high doping levels and reduced gate dielectric thicknesses the normal electric field increases significantly, and quantum mechanical effects become more pronounced [3].

1.3 Review of past and present works on Quantization effects on threshold voltage

The quantum nature of the two-dimensional electron gas in MOSFETs has been studied in detail and is a well-established fact [4], but a full quantum-mechanical (QM) treatment is difficult, time consuming and for silicon MOSFETs hardly ever necessary. But with high doping levels and decreased oxide layer thicknesses QM effects become noticeable and a pure classical description of the physics is not sufficient for an accurate calculation of the inversion layer charges.

The numerical self-consistent calculation of energy subbands of silicon inversion layers has been carried out in [4]. Recently, a simple and approximate model has been proposed [5]. There the average inversion layer depth calculated quantum mechanically was compared with the classical calculation and the difference between the two were transferred into the classical calculation through the modification of the gate oxide thickness.

1.4 Objective of this work

With increased channel doping and reduced gate oxide thickness required in scaled devices the quantum mechanical treatment of the inversion layer of MOSFETs has become necessary. The inversion region charge concentration and distribution is different when quantum mechanical phenomena is taken into account. In this work we treat the electric quantum limit, in which only the lowest electric subband is occupied. Mathematical expressions for the lowest energy subband and the average separation of carriers from the semiconductor-insulator interface will be carried out and the derived expressions will be used to establish a relation between the surface potential

and the threshold voltage. An algorithm will be developed to study the results predicted by the above relations. Therefore, the main objective of this research is to develop a computer efficient analytical model for determining the threshold voltage of low dimensional MOSFETs incorporating the quantization effects.

1.5 Summary of the thesis.

In this thesis, Schrödinger wave equation for the two-dimensional inversion layer carriers is solved approximately incorporating proper boundary conditions. The effects of quantization on inversion layer carriers and the spatial distribution of carriers inside the potential well is studied here. An analytical model for threshold voltage is also developed to calculate the quantum threshold voltage computer efficiently.

Schrödinger wave equation is solved using WKB approximate method. WKB method and its application on MOSFETs is discussed in chapter 2. Also an analytical model to calculate quantum threshold voltage is developed here.

The analytical model developed in chapter 2 is used to determine the threshold voltage of a MOSFET for different channel doping levels and oxide layer thicknesses. The results of the quantum mechanical effects on various MOSFET parameters including quantum threshold voltage are given in chapter 3.

Chapter 4 contains the concluding remarks along with recommendations for future work on this topic.

CHAPTER 2

MATHEMATICAL ANALYSIS FOR THRESHOLD VOLTAGE OF MOSFETS UNDER INVERSION CONSIDERING QUANTIZATION EFFECTS

2.1 Introduction

At increased channel doping levels and reduced gate oxide thicknesses the inversion layer carriers are confined in a potential well near the Si/SiO_2 interface. At high doping levels, the width of the potential well becomes comparable to the de Broglie wavelength of the inversion layer carriers and quantum mechanical effects become pronounced. As a result, the bulk conduction band is split into discrete subbands in the inversion layer with the lowest subband shifted substantially above the conduction band minimum. The effects of quantization can be most accurately modeled by solving the Schrödinger's and

Poisson's equations self-consistently. But this approach involves much computational time. On the other hand, a simpler approach to model the quantization effects is to determine analytically the lowest allowed eigen-energy and electron population in the energy sub-bands. In this work we treat the electric quantum limit, in which only the lowest electric subband is occupied. Due to the quantum nature of the electric population of the energy subband their average penetration into the semiconductor is greater than the classical treatment.

In this chapter WKB (Wentzel-Kramers-Brillouin) approximation technique is used to find an analytical expression for the energy subbands of MOSFETS under inversion. Also due to the quantum mechanical nature of the confined inversion layer carriers, they are spatially shifted from the Si/SiO_2 interface. Here an analytical expression for average separation of carriers from the Si/SiO_2 interface is also determined using the results of the WKB method. Finally an analytical model is developed using the expressions of the lowest energy subband and the average penetration of the carriers from the Si/SiO_2 interface to determine the threshold voltage of MOSFETs. This quantum threshold voltage is compared with the classical threshold voltage to justify the validity of the analytical model.

2.2. WKB Approximation

2.2.1 Introduction

This is an approximate method of solution of ordinary differential equations. The basis of the method is an expansion of the wave function in powers of h/2π, which, although of a semiconvergent or asymptotic character, is nevertheless also useful for the approximate solution of quantum-mechanical problems in appropriate cases. Its utility is expected to be highest in situations were h/2π can be considered small and is often referred to as the semi-classical approximation (since classical mechanics corresponds to h/2π → 0.0).

2.2.2 The One-Dimensional Schrödinger wave equation

The solution of the Schrödinger wave equation

$$i\hbar \frac{\delta \psi}{\delta t}(r,t) = -\frac{\hbar^2}{2m} \nabla^2 \psi(r,t) + V(r) \psi(r,t) \quad (2.1)$$

can be written in the form [6]

$$\psi(r,t) = A\, e^{\frac{iW(r,t)}{\hbar}} \qquad (2.2)$$

in which case W satisfies the equation

$$\frac{\delta W}{\delta t} + \frac{1}{2m}(\nabla W)^2 + V(r) - \frac{i\hbar}{2m}\nabla^2 W = 0 \qquad (2.3)$$

if $\psi(r,t)$ is an energy eigenfunction

$$\psi(r,t) = \mu(r)\, e^{-\frac{iEt}{\hbar}} \qquad (2.4)$$

where E is the energy of the particle. Now W can be written using (2.2) and (2.4) as

$$W(r,t) = S(r) - Et \qquad (2.5)$$

where

$$u(r) = A\, e^{\frac{iS(r)}{\hbar}} \qquad (2.6)$$

substituting (2.5) into (2.3) gives

$$\frac{1}{2m}(\nabla S)^2 - [E - V(r)] - \frac{i\hbar}{2m}\nabla^2 S = 0 \qquad (2.7)$$

2.2.3 Approximate solutions

let us define

$$k(x) = \frac{\sqrt{2m[E - V(x)]}}{\hbar} \qquad when \quad V(x) < E \qquad (2.8)$$

and

$$\rho(x) = \frac{\sqrt{2m[V(x) - E]}}{\hbar} \qquad when \quad V(x) > E \qquad (2.9)$$

The basic equation that we consider is written in one of the forms:

$$\frac{d^2u}{dx^2} + k^2(x)\,u = 0 \qquad k^2 > 0 \qquad (2.10)$$

and

$$\frac{d^2u}{dx^2} - \rho^2(x)\,u = 0 \qquad \rho^2 > 0 \qquad (2.11)$$

First we consider (2.10). For one dimensional analysis we write (2.6) as

$$u(x) = A\,e^{\frac{iS(x)}{\hbar}} \qquad (2.12)$$

substituting (2.12) into (2.10) gives

$$i\hbar S''(x) - [S'(x)]^2 + \hbar^2 k^2(x) = 0 \qquad (2.13)$$

where primes denote differentiation with respect to x.

We substitute expansion of S in powers of h/2π and equate equal powers of h/2π.

$$S = S_0 + \hbar S_1 + \hbar^2 S_2 + \ldots \tag{2.14}$$

$$-S_0'^2 + 2m(E - V) = 0 \tag{2.15}$$

$$iS_0'' - 2S_0'S_1' = 0 \qquad etc \tag{2.16}$$

Integrating (2.15) and 2.16) gives

$$S_0(x) = \pm \int^x k(x)\ dx \tag{2.17}$$

$$S_1(x) = \frac{1}{2}\, i \ln k(x) \tag{2.18}$$

where arbitrary constants of integration that can be absorbed in the coefficient A have been omitted. Substitution of (2.17) and (2.18) into (2.12) results in

$$u(x) = Ak^{-\frac{1}{2}} \exp(\pm i \int^x k\ dx) \qquad V<E \tag{2.19}$$

Similarly, the approximate solution of (2.11) is

$$u(x) = B\rho^{-\frac{1}{2}} \exp(\pm \int^x \rho\ dx) \qquad V>E \tag{2.20}$$

2.2.4 Solution near a turning point

A turning point is a point at which E-V(x) = 0; on approaching such point, the kinetic energy (E-V) of a classical particle decreases to zero, and it has to turn back. Let us consider a particular turning point occurring for a given energy E. We can take the origin of the x coordinate at this point, without loss of generality, so that (E-V)=0 at x=0. We also assume for the moment that V(x) < E to the right of the turning point (Positive x) and put

$$\xi(x) \equiv \int_0^x k\,dx \tag{2.21}$$

Now if

$$k^2(x) = cx^n \tag{2.22}$$

where C is a positive constant, then (2.10) has the solution of the form

$$u(x) = A\xi^{\frac{1}{2}}k^{-\frac{1}{2}}J_{\pm m}(\xi) \tag{2.23}$$

where

$$m = \frac{1}{n+2} \tag{2.24}$$

and J is a Bessel function of order m.

2.2.5 Linear turning point

Let us now consider the most commonly occurring situation, of a linear turning point, i.e. one near which the variation of (E-V) or K^2 with x is linear (Fig.2.1). This corresponds to taking n = 1 in (2.22). Here (2.10) is used in region 1 (x>0) and (2.11) in region 2 (x<0). We make the following definitions:

$$\text{For} \quad x > 0 \qquad \xi_1 \equiv \int_0^x k \, dx \qquad (2.25)$$

$$\text{For} \quad x < 0 \qquad \xi_2 \equiv \int_0^x \rho \, dx \qquad (2.26)$$

Both ξ_1 and ξ_2 are real and positive, and increase with distance from the turning point. The two independent solutions in each of the two regions are:

$$u_1^{\pm}(x) = A_{\pm} \, \xi_1^{\frac{1}{2}} k^{-\frac{1}{2}} J_{\pm\frac{1}{3}} \, (\xi_1) \qquad (2.27)$$

$$u_2^{\pm}(x) = B_{\pm} \, \xi_2^{\frac{1}{2}} \rho^{-\frac{1}{2}} I_{\pm\frac{1}{3}} \, (\xi_2) \qquad (2.28)$$

where in (2.28) J is replaced by I, the Bessel function of imaginary argument.

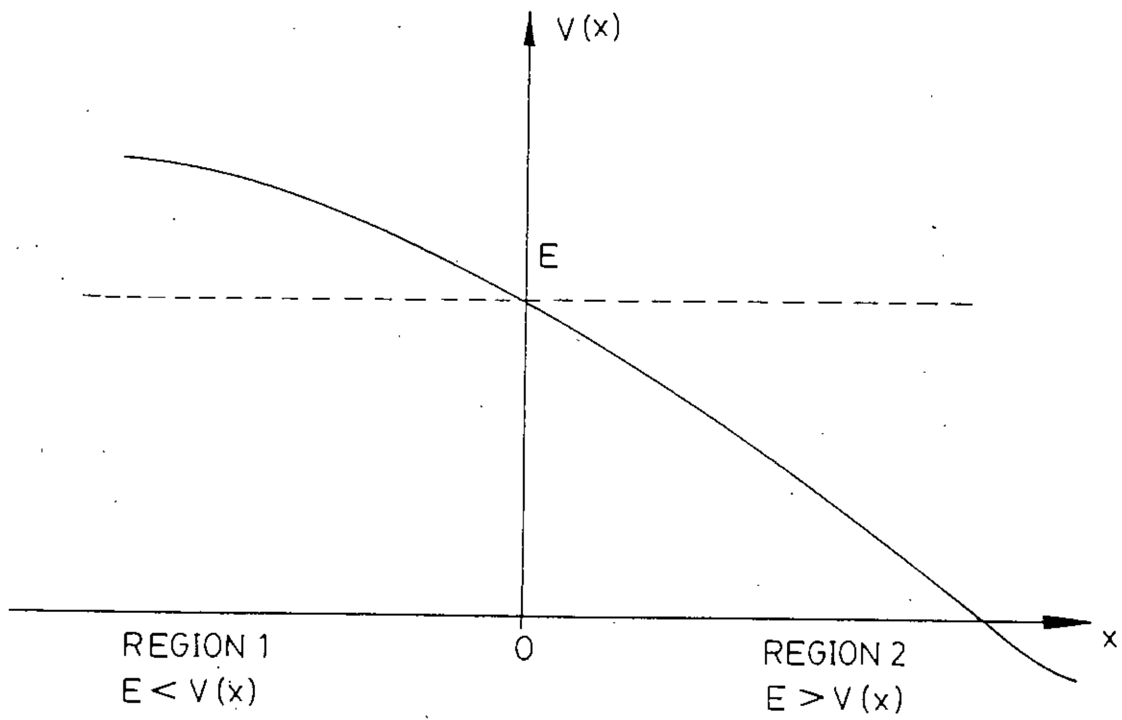

Fig. 2·1 Linear turning point.

We require the leading terms of the power series expansions and of the asymptotic expansions for these functions [6]

$$J_{\pm\frac{1}{3}}(\xi_1) \xrightarrow[x\to 0]{} \frac{(\frac{1}{2}\xi_1)^{\pm\frac{1}{3}}}{\Gamma(1\pm\frac{1}{3})}$$

$$\xrightarrow[x\to\infty]{} (\tfrac{1}{2}\pi\xi_1)^{-\frac{1}{2}} Cos(\xi_1 \mp \frac{\pi}{6} - \frac{\pi}{4})$$

(2.29)

$$I_{\pm\frac{1}{3}}(\xi_2) \xrightarrow[x\to 0]{} \frac{(\frac{1}{2}\xi_2)^{\pm\frac{1}{3}}}{\Gamma(1\pm\frac{1}{3})}$$

$$\xrightarrow[x\to\infty]{} (2\pi\xi_2)^{-\frac{1}{2}} (e^{\xi_2} + e^{-\xi_2} e^{-(\frac{1}{2}\pm\frac{1}{2})\pi i})$$

2.2.6 Connection at the turning point

To match u_1 and u_2 at x=0, we need to known their behavior near this point. The leading term in K^2 at x=0 is Cx so that

$$k \approx c x^{1/2}, \; \rho \approx c|x|^{1/2}, \; \xi_1 \approx \left(\frac{2c}{3}\right) x^{\frac{3}{2}}, \; \xi_2 \approx \left(\frac{2c}{3}\right) |x|^{\frac{3}{2}}$$

$$\text{where} \qquad c = +C^{\frac{1}{2}} \tag{2.30}$$

Then from (2.27), (2.28) and (2.29) we obtain the behavior of the u's near x = 0 :

$$u_1^+ \approx A_+ \frac{\left(\frac{2}{3}\right)^{\frac{1}{2}} \left(\frac{1}{3}c\right)^{\frac{1}{3}}}{\Gamma\left(\frac{4}{3}\right)} x \qquad u_1^- \approx A_- \frac{\left(\frac{2}{3}\right)^{\frac{1}{2}} \left(\frac{1}{3}c\right)^{-\frac{1}{3}}}{\Gamma\left(\frac{2}{3}\right)}$$

$$(2.31)$$

$$u_2^+ \approx B_+ \frac{\left(\frac{2}{3}\right)^{\frac{1}{2}} \left(\frac{1}{3}c\right)^{\frac{1}{3}}}{\Gamma\left(\frac{4}{3}\right)} |x| \qquad u_2^- \approx B_- \frac{\left(\frac{2}{3}\right)^{\frac{1}{2}} \left(\frac{1}{3}c\right)^{-\frac{1}{3}}}{\Gamma\left(\frac{2}{3}\right)}$$

It is clear from this that u_1^+ joins smoothly on to u_2^+ if $B_+=-A_+$ and that u_1^- joins smoothly on to U_2^- if $B_-=-A_-$.

These relations between the coefficients can be used to obtain asymptotic forms like (2.19) and (2.20) for the two independent solutions u^+ and u^- in the two regions (the arbitrary multiplying constants A± are omitted).

$$u^+ \xrightarrow[x\to+\infty]{} (\tfrac{1}{2}\pi k)^{-\frac{1}{2}} Cos\,(\xi_1 - \frac{5\pi}{12}) \qquad (2.32a)$$

$$\xrightarrow[x\to-\infty]{} -(2\pi\rho)^{-\frac{1}{2}} \,(e^{\xi_2} + e^{-\xi_2} - \frac{5\pi i}{6}) \qquad (2.32b)$$

$$u^- \xrightarrow[x\to+\infty]{} (\tfrac{1}{2}\pi k)^{-\frac{1}{2}} Cos\,(\xi_1 - \frac{\pi}{12}) \qquad (2.32c)$$

$$\xrightarrow[x\to-\infty]{} (2\pi\rho)^{-\frac{1}{2}} \,(e^{\xi_2} + e^{-\xi_2} - \frac{\pi i}{6}) \qquad (2.32d)$$

2.2.7 Asymptotic connection formulas

By forming suitable linear combinations of the independent solutions u^+ and u^- we can form particular solutions with specified asymptotic properties in either of the regions ($x>0$ or $x<0$) and can find the behavior of the solution in the other region.

From (2.32b) and (2.32d) it is evident that it is the combination ($u^+ + u^-$) which decreases exponentially on going into the interior of the classically forbidden region ($x\to\infty$); on noting its asymptotic form as $x\to+\infty$ from (2.32a) and (2.32c) we see that it behaves like $K^{-\frac{1}{2}}\ Cos(\xi_1 - \pi/4)$. Thus, we have the first connection formula from the asymptotic region $x\to-\infty$ to the region $x\to+\infty$.

$$\frac{1}{2}\rho^{-\frac{1}{2}}e^{-\xi_2} \longrightarrow K^{-\frac{1}{2}}\cos(\xi_1 - \frac{\pi}{4}) \qquad (2.33)$$

The formula is not valid in the reverse direction, since a slight error in the phase of the cosine function is enough to introduce a small admixture of the exponentially increasing function, which will overwhelm $e^{-\xi_2}$ for large negative x values.

Another linear combination of u^+ and u^- gives the second connection formula

$$Sin\,\eta\,\rho^{-\frac{1}{2}}e^{-\xi_2} \longleftarrow K^{-\frac{1}{2}}\cos(\xi_1 - \frac{\pi}{4} + \eta) \qquad (2.34)$$

where η is appreciably different from zero or an integer multiple of π. Once again the formula holds only in the direction indicated by the arrow, since a small admixture of the $e^{-\xi_2}$ term on the left hand side is enough to change the phase on the right hand side drastically.

2.3 Eigen energy of a Triangular potential well.

We require the wave function to vanish at the Si/SiO_2 interface, where z=0. This should be a good approximation for

the Si/SiO_2 interface for which the potential barrier for electrons is approximately 3 eV.

In most cases of interest for Si, the depletion layer is much wider than the inversion layer. The inversion layer is even narrower for high channel doping levels, so that the electrostatic potential V(z) (in the z direction) from the interface is assumed to have a triangular form (a triangular potential well approximation). At the interface the potential is assumed to be infinite (Fig.2.2) i.e.,

$$\begin{aligned} V(z) &= \infty, \qquad & z \le 0 \\ &= eF_s z, \qquad & z \ge 0 \end{aligned} \tag{2.35}$$

where F_S is the electric field perpendicular to the interface. One of the turning points is Z=0, and the other one follows from the equation $V(z=b) = eF_S b = E$

$$b = \frac{E}{eF_s} \tag{2.36}$$

For a potential trough (Fig.2.3) in the semi-classical expressions for the wave function the phase starts in both turning points at $\pi/4$.

The connection formula (2.33) can be applied at the turning point z=a, which separates a type 2 region from the

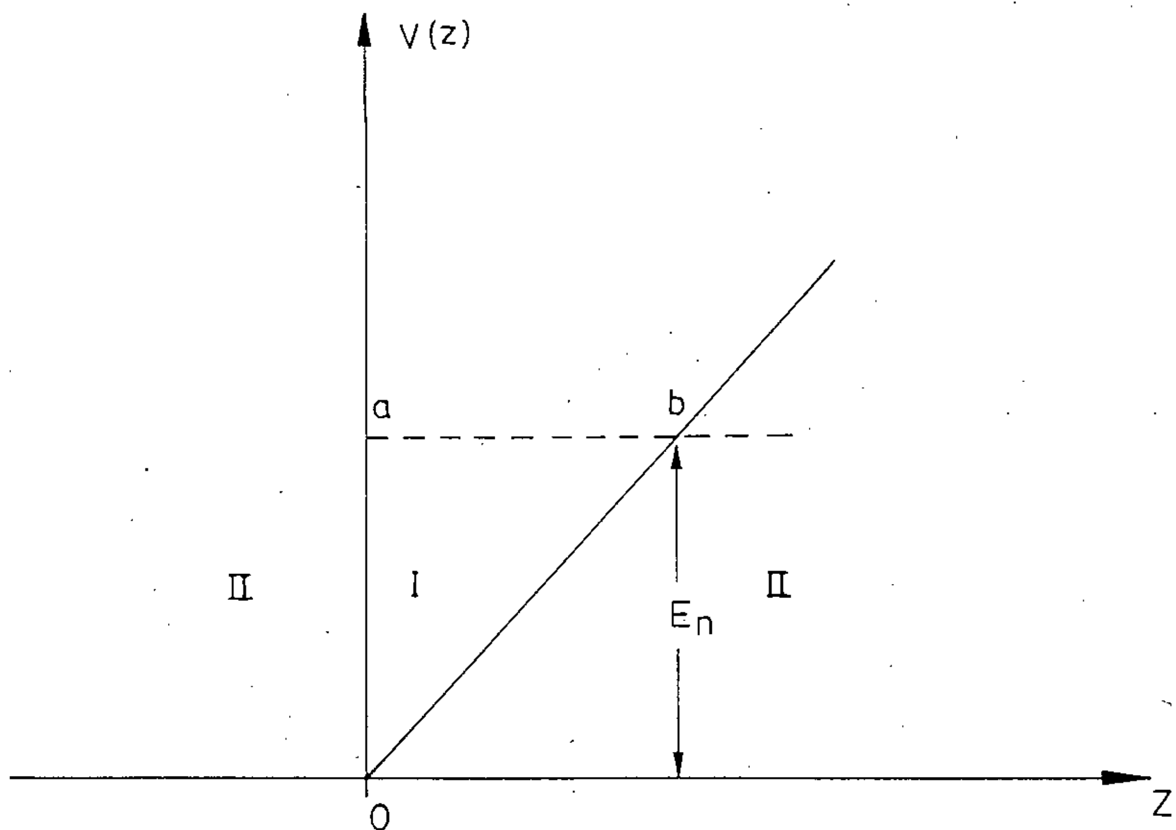

Fig. 2.2 Electrostatic potential well.

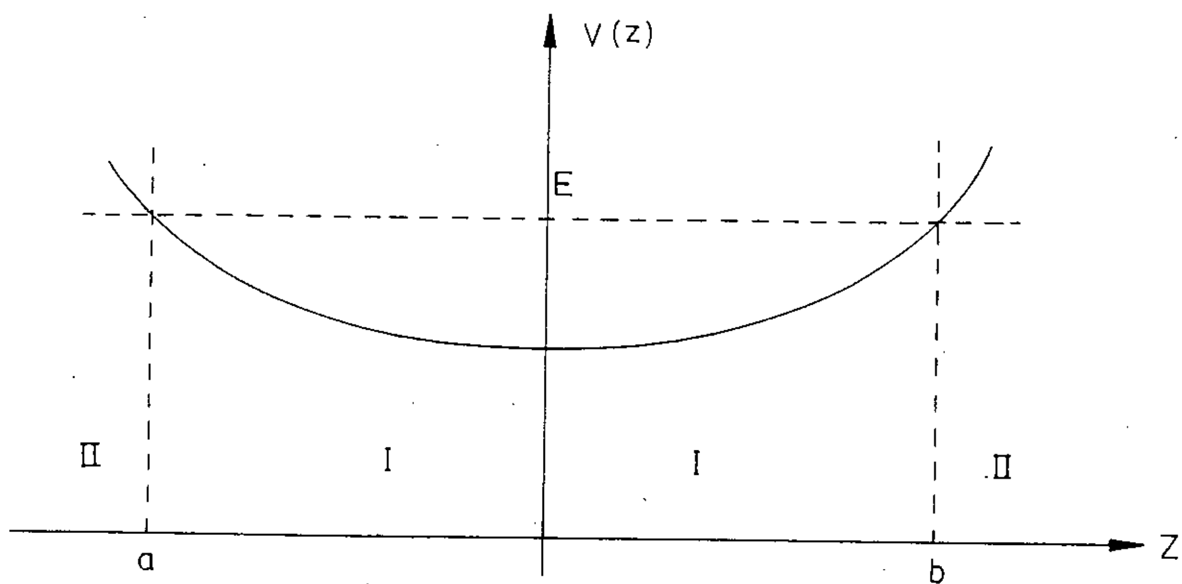

Fig. 2.3 Potential trough.

type 1 region $a<z<b$. The only change is that the lower limit on the ξ_1 integral is changed from 0 to a, so that the solution to the right of the turning point is

$$k^{-\frac{1}{2}} Cos \left(\int_a^z k\, dz - \frac{\pi}{4}\right) \quad (2.37)$$

apart from an arbitrary multiplying constant. Here, the turning point z=a=0 corresponds to a "vertical potential wall" so that the wave function must vanish at z=0 and the phase should be zero. As a result (2.37) does not start with a term $\pi/4$, instead it must start with phase zero at z=0. Hence the solution to the right of z=0 is

$$k^{-\frac{1}{2}} Cos \left(\int_a^z k\, dz - \frac{\pi}{4} - \frac{\pi}{4}\right)$$

$$= k^{-\frac{1}{2}} Cos \left(\int_a^z kdz - \frac{\pi}{2}\right) \quad (2.38)$$

The same connection formula can also be applied at z=b by reversing the direction of the x axis and changing the fixed limit on the ξ integral from 0 to b. We redefine

$$\xi_1 = \int_z^b k\, dx, \quad \xi_2 = \int_b^z \rho\, dx \quad (2.39)$$

So that they still increase going away from the turning point.

The solution to the left of this turning point is then

$$k^{-\frac{1}{2}} Cos\,(\int_z^b k\,dx - \frac{\pi}{4}) \qquad (2.40)$$

Which can be written as

$$k^{-\frac{1}{2}} Cos\,(\int_a^z k\;dx - \frac{\pi}{4} - \eta)$$

$$= k^{-\frac{1}{2}} Cos\,\{\int_a^z kdx - \frac{\pi}{2} - (\eta - \frac{\pi}{4})\} \qquad (2.41)$$

where

$$\eta \equiv \int_a^b k\;dx - \frac{\pi}{2} \qquad (2.42)$$

For the two solutions (2.38) and (2.41) to join smoothly in the interior of region 1, the arguments of the cosine terms must be equal. Hence the condition here is

$$\eta - \frac{\pi}{4} = n\pi \quad , \eta = 0,\ 1,\ 2, \ldots \qquad (2.43)$$

Using (2.42) and rearranging we get

$$\int_a^b \frac{\sqrt{2m[E_n - V(z)]}}{\hbar}\,dz = (n + \frac{3}{4})\,\pi \qquad (2.44)$$

Putting the value a=0 and $b=E/eF_s$ and integrating we get

$$E_n = \left(\frac{\hbar^2}{2m}\right)^{\frac{1}{3}} \left[\frac{3}{2}\pi e F_s \left(n+\frac{3}{4}\right)\right]^{\frac{2}{3}} \qquad (2.45)$$

This is the analytical expression for energy subbands in the inversion layer of MOSFETS.

In the electric quantum limit, when only the lowest energy level is occupied a general solution for all kinds of semiconductors and possible orientations of the surface can be obtained [7]. Hence, we take n=0 in (2.45) and use the resulting lowest energy level for future calculations. The lowest energy level of the triangular potential well is then given by

$$E_o = \left(\frac{\hbar^2}{2m}\right)^{\frac{1}{3}} \left(\frac{9}{8} e\pi F_s\right)^{\frac{2}{3}} \qquad (2.46)$$

Now, in the MOSFET structure the width of the inversion layer is in the nanometer range for high substrate doping levels. In this narrow range of inversion layer width the electrostatic potential of the well can be assumed to be triangular. On the other hand the depth of the potential well at the Si/SiO_2 interface is more than several electron volts, so that it may virtually be treated as an infinite potential barrier. Furthermore, the electric field normal to the Si/SiO_2 interface is assumed to be constant in the narrow potential well. Consequently the results of the triangular potential well can be used in the inversion layer of the heavily doped MOSFETs.

2.4 Average separation of minority carriers.

From (2.38) we get the solution of the Schrödinger wave equation inside the potential well given by

$$u(z) = ck^{-\frac{1}{2}} \, Sin\left(\int_a^z k \, dz\right) \qquad (2.47)$$

Using equation (2.8) and integrating within the limit z=b we find

$$\begin{aligned} \int_a^z k \, dz &= \frac{2\sqrt{2m}}{3\hbar^2} E_n^{\frac{1}{2}} z \\ &= Az \end{aligned} \qquad (2.48)$$

where

$$A = \frac{2\sqrt{2m}}{3\hbar^2} \, E_n^{\frac{1}{2}} \qquad (2.49)$$

Since the solutions produce a standing wave inside the potential well we approximate Sin(AZ) = ½ inside the well. Now using (2.8) again (2.47) becomes

$$u(z) = \frac{1}{2} c\hbar \left[2m(E_n - eF_s z)\right]^{-\frac{1}{4}} \qquad (2.50)$$

The average separation of carriers, (Fig.1.5), from the Si/SiO_2 is then found by using

$$Z_{av} = \langle z \rangle = \frac{\int_0^b z u(z) \, dz}{\int_0^b u(z) \, dz} \qquad (2.51)$$

Substituting the value of (2.50) into (2.51) and performing the integration we get

$$Z_{av} = \frac{4}{7}\frac{E_n}{eF_s} \qquad (2.52)$$

This is the required separation of carriers from the Si/SO_2 interface.

2.5 Quantum Threshold Voltage.

To determine the quantum threshold voltage of MOSFETs, the classical definition of threshold voltage is applied here.

Classically at $\psi_S=\psi_{Si}$ inversion layer carriers are negligible compared to the depletion region ionized acceptors. The surface potential due to depletion region ionized acceptors is given by

$$\Phi_d = \frac{eN_A Z_d^2}{2\epsilon_s} \qquad (2.53)$$

where Z_d is the depth of the depletion region charge. The concentration of electrons at any distance Z perpendicular to the interface into the semiconductor is given by

$$n(z) = n_i e^{\frac{q}{kt}(\psi-\Phi_F)} \qquad (2.54)$$

If ψ is replaced by ϕ_d, (2.53), and Z_d by Z and also if the condition that n(z=o)=N_A is applied for $\psi = \psi_S$, then we get

$$n(z) = N_A e^{-\frac{eN_A}{2\epsilon_s V_T}Z^2} \qquad (2.55)$$

Integrating (2.55) from Z=O to Z=∞ results in the total concentration of electrons per meter square in the inversion region given by

$$N_{inv} = \left(\frac{\pi e_s V_T N_A}{2e}\right)^{\frac{1}{2}} \qquad (2.56)$$

This total electron concentration and the total impurity ions N_{depl} can be used in the quantum mechanical calculations to find the electric field perpendicular to the Si/SiO_2 interface. The electric field at the interface is given by

$$F_s = \frac{eN_T}{e_s} = \frac{e\,(N_{inv} + N_{depl})}{e_s} \qquad (2.57)$$

where $N_T=N_{inv}+N_{depl}$ and N_{depl} is given by (1.7). ϵ_s is the permittivity of silicon.

Using the calculated electric field in (2.46) and (2.52) the first energy subband and average separation of carriers from the Si/SO_2 interface can be determined.

For a two-dimensional density of states given by D for energies greater than E_0 is given by Fermi-Dirac statistics

$$N_{inv} = D\int_{E_o}^{\infty} \frac{dE}{1 + e^{\frac{q}{kt}(E-E_F)}} \qquad (2.58)$$

Applying the easily verifiable formula

$$\int \frac{dx}{1 + e^{x}} = -\ln\,(1 + e^{-x}) \qquad (2.59)$$

we get,

$$N_{inv} = D\frac{kt}{q}\ln\left[1 + e^{\frac{q}{kt}(E_F - E_o)}\right] \tag{2.60}$$

where, D is the density of states associated with a single quantized energy level for a 2D system given by

$$D = \frac{e m_d n_v}{\pi \hbar^2} \tag{2.61}$$

where n_v and m_d are the valley degeneracy and the density-of-state effective mass per valley.

The band bending ϕ_d is associated with the depletion layer charge (Fig.2.4). When an inversion layer has formed, the band bending ϕ_d is given approximately by

$$e\Phi_d \cong (E_c - E_F)_b \tag{2.62}$$

the energy difference between the bottom of the conduction band in the bulk and the Fermi level. There are several corrections to this value. We have assumed that the depletion charge is constant for a distance Z_d, the depletion layer width, from the surface and then goes abruptly to zero. This assumption fails in the transition region from depletion to bulk, in which the field decays to zero exponentially with a characteristic distance given by the bulk screening length. The correction to $e\phi_d$ is given in [8] to be equal to -kT, so that (2.62) can be written as

$$e\Phi_d = (E_c - E_F)_b - kT$$

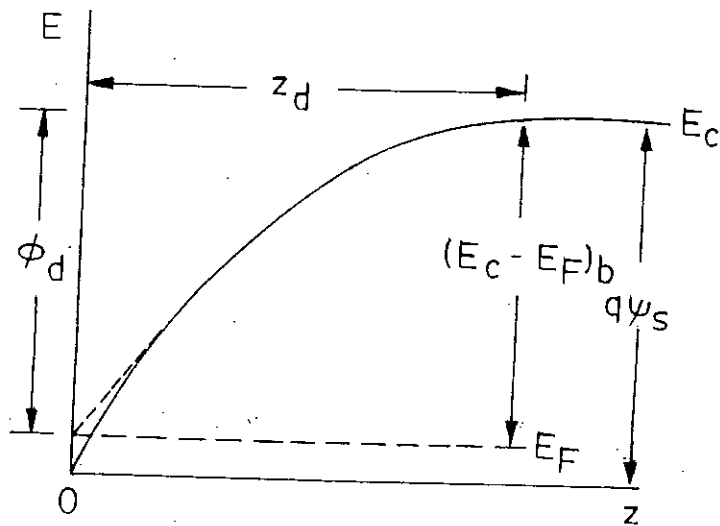

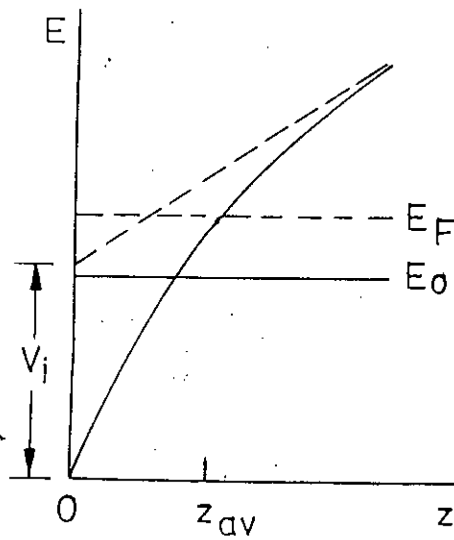

Fig. 2.4 Band bending due to depletion charges.
(a) Surface potential ψ_s and band bending
(b) Potential drop due to inversion charges

The surface potential ψ_s arises from the contribution of both the depletion and inversion layer charges. Since the bottom of the conduction band is taken as zero at the Si/SiO_2 interface we have

$$e\psi_s = (E_c - E_F)_b + E_F$$

Now, the contribution of inversion layer electrons to the surface potential can be written as

$$V_i = \frac{e N_{inv} Z_{av}}{\epsilon_s}$$

where, N_{inv} is the total concentration of inversion layer electrons taking quantum-mechanical effects into account and Z_{av} is their average distance from the semiconductor-insulator interface. Therefore, the band bending ϕ_d associated with depletion layer charges can be written as

$$e\phi_d = [(E_c - E_F)_b + E_F - kt] - V_i \qquad (2.63)$$

The last term in (2.63) is the potential drop V_i across the inversion layer.

The depletion layer width can be calculated by

$$Z_d = \sqrt{\frac{2\epsilon_s\phi_d}{eN_A}} \qquad (2.64)$$

and the carrier concentration is given by

$$N_{depl} = Z_d N_A \qquad (2.65)$$

An one-dimensional searching algorithm, which is developed in chapter three, is used to calculate N_{inv}, E_F, ψ_S, ϕ_d, Z_d and N_{depl}. Then the quantum threshold voltage can be computed by

$$V_T \equiv V_G = V_{ox} + e\psi_s \qquad (2.66)$$

where,

$$V_{ox} = \frac{\epsilon_s F_s t_{ox}}{\epsilon_{ox}} \qquad (2.67)$$

is the oxide layer voltage drop, F_s is the normal electric field, t_{ox} is the oxide layer thickness and ϵ_{ox} is the permittivity of the oxide.

2.6 Summary

WKB approximation is used in this chapter to solve the Schrödinger wave equation inside the triangular potential well formed within the inversion layer of MOSFETs. Electrostatic potential inside the narrow well is assumed to be triangular in shape and the electric field normal to the Si/SiO_2 is assumed to be constant inside the well. Appropriate boundary conditions are used to determine the mathematical expression for the Eigen energy of the various subbands inside the well. Then the solution of the Schrödinger wave equation is used to determine the mathematical expression for the average separation of minority carriers from the $SiSO_2$ interface inside the triangular potential well. Finally an analytical model is

developed to calculate the quantum threshold voltage using an iterative method. Classical threshold voltage is also calculated to study the threshold voltage shift due to quantum mechanical effects.

CHAPTER 3

RESULTS BASED ON ANALYTICAL SOLUTION

3.1 Introduction

The MOS device is studied in this work using computational method. The analytical solution of the MOSFET incorporating quantum mechanical effects into account are compared with the classical results. One dimensional searching algorithm is used in the computational method and the MOS device is studied for different channel doping levels and oxide layer thicknesses. The lowest allowed energy level shift, the variation of inversion and depletion layer charge concentration, the variation of the average penetration of inversion layer charge from the Si/SiO_2 interface and the threshold voltage shift due to quantum mechanical calculation are particularly studied here.

3.2 Computational method in studying MOS device

The classical concentration of minority carriers is calculated using (2.56). The electric field perpendicular to the

Si/SiO_2 interface is then calculated using (2.57). An one dimensional searching algorithm is used to determine the inversion and depletion layer minority carrier charge concentration and the electric field produced by the sum of them is compared with (2.57). If the two electric fields matches then the searching algorithm comes to an end. In this process we also get the corresponding Fermi energy level, surface potential, potential due to depletion layer charge and depletion region width. The quantum threshold voltage is calculated by (2.66) and the classical threshold voltage is determined using (2.10).

3.3 Results and discussions

3.3.1 Energy level shift

The predicted difference between the energy level of the lowest sub-band (E_0) and the bottom of the conduction band (E_c) increases as the surface potential is increased (Fig.3.1). The difference between the two increases as the device becomes more strongly inverted. The variation of energy level shift with inversion layer charge is shown in (Fig.3.2). Since the lowest allowed energy level has an energy above the bottom of the conduction band, the effective silicon bandgap in the inversion layer may be treated with a bandgap widening model. The amount of widening is simply the difference in the energy between the bottom of the conduction band E_c , and the first allowed energy

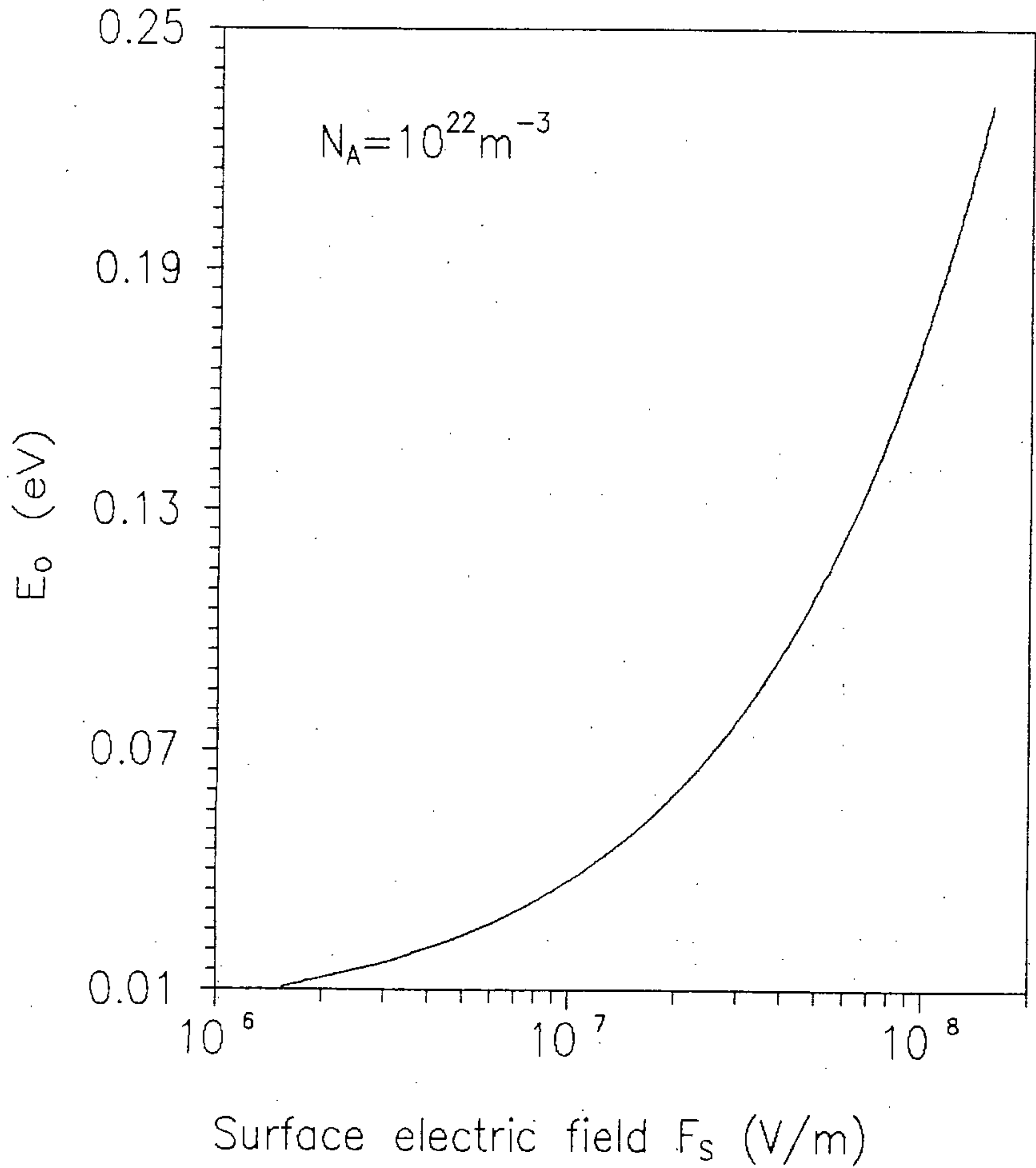

Fig. 3.1 Effect of surface electric field on the lowest energy subband.

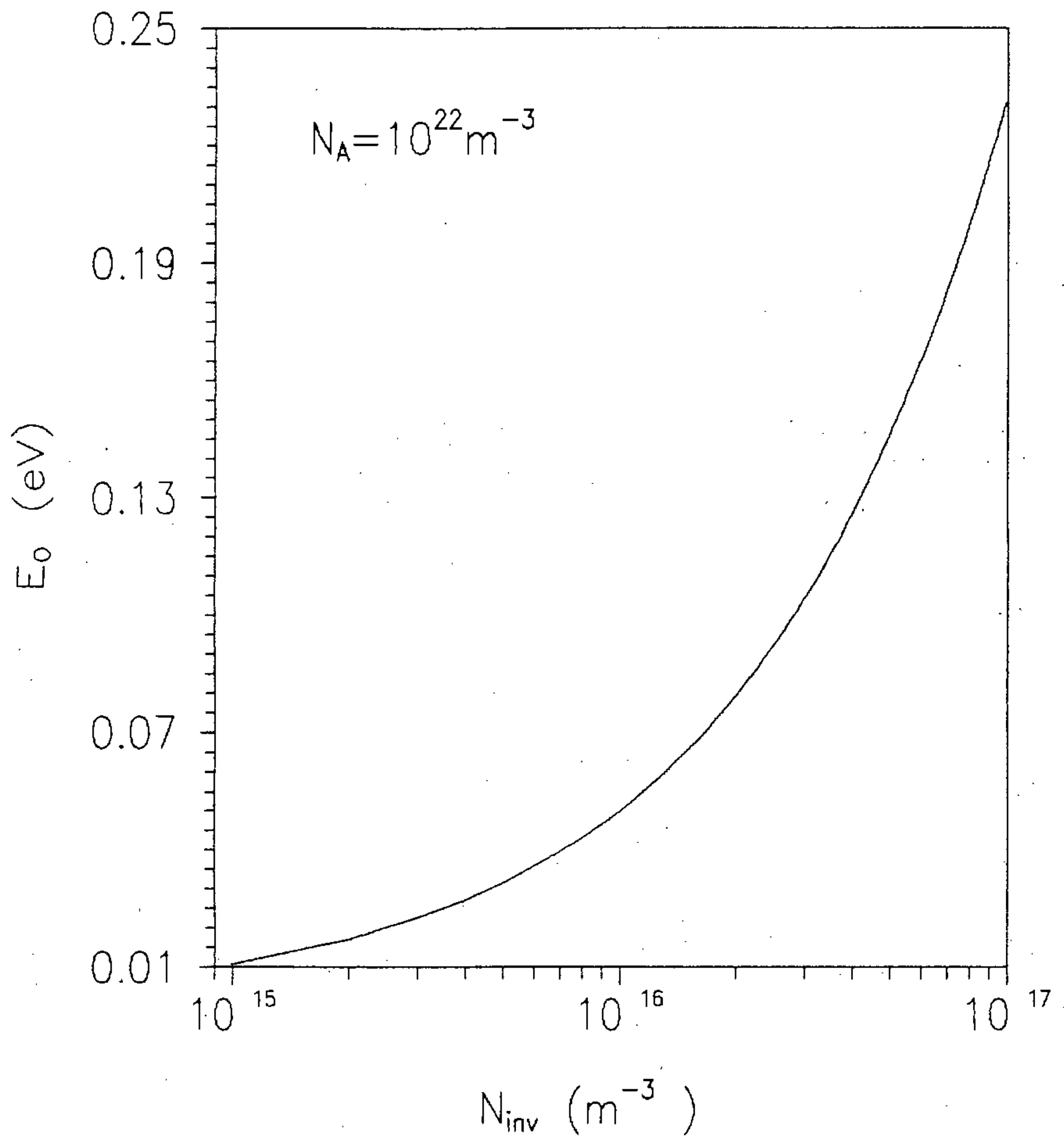

Fig. 3.2 Lowest energy subband vs. inversion layer charge.

level, E_0. Therefore, if E_g is the bandgap, the increase in the bandgap due to quantization is given as,

$$\Delta E_g = E_g^{QM} - E_g^{Classical} = E_o - E_c \tag{3.1}$$

It is convenient to model the apparent bandgap increase as a decrease in the local effective intrinsic concentration. Therefore, the new quantum mechanical effective intrinsic carrier concentration $n_{i_{eff}}$ is given by,

$$n_{i_{eff}}^{QM} = n_{i_{eff}}^{Classical} \times e^{\left(\frac{-\Delta E_g}{2kT}\right)} \tag{3.2}$$

in which $n_{i_{eff}}^{Classical}$ is the conventional model for the intrinsic carrier concentration. Therefore, the lowest allowed energy level E_0 can be used as a parameter to model the effect of the inversion layer quantization on the inversion charge density of the MOS device.

3.3.2 Inversion layer charge concentration

From (Fig.3.3) it can be seen that the quantum mechanical inversion layer charge concentration varies considerably as the surface potential i.e., gate voltage increases. Inversion layer quantization decreases the rate at which the inversion layer

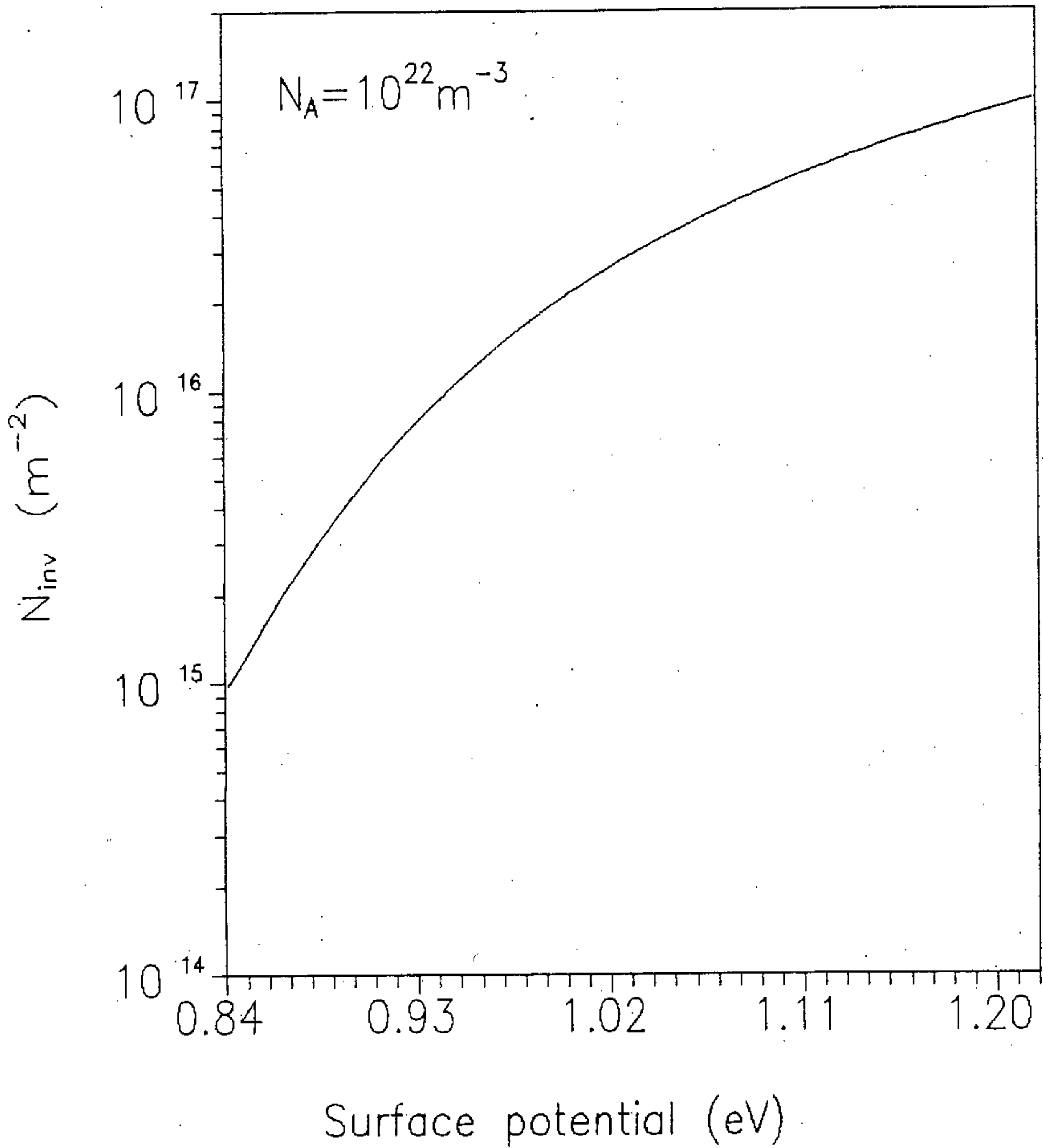

Fig. 3.3 Effect of surface potential on inversion layer charge.

charge density increases with gate voltage. But the inversion layer charge density is dependent on the lowest allowed energy level (Fig.3.2). Therefore, it is again evident that the lowest allowed energy level can actually be used as a parameter to model the effects of quantization on the inversion layer charge density.

3.3.3 Depletion layer charge concentration

As can be seen from (Fig.3.4) and (Fig.3.5) the variation of depletion layer charge concentration is very small compared to the inversion layer charge concentration. Once strong inversion occurs, the depletion-layer width reaches a maximum i.e., When the bands are bent down far enough such that $\psi_s = \psi_{si}$, the semiconductor is effectively shielded from further penetration of the electric field by the inversion layer carriers and even a very small increase in band bending (corresponding to a very small increase in the depletion-layer width) results in a very large increase in the charge density within the inversion layer. Therefore, after some value of gate voltage depletion layer charge concentration becomes almost constant.

3.3.4 The average penetration of the inversion-layer charge density from the surface

From (Fig.3.6) we observe that the average penetration of

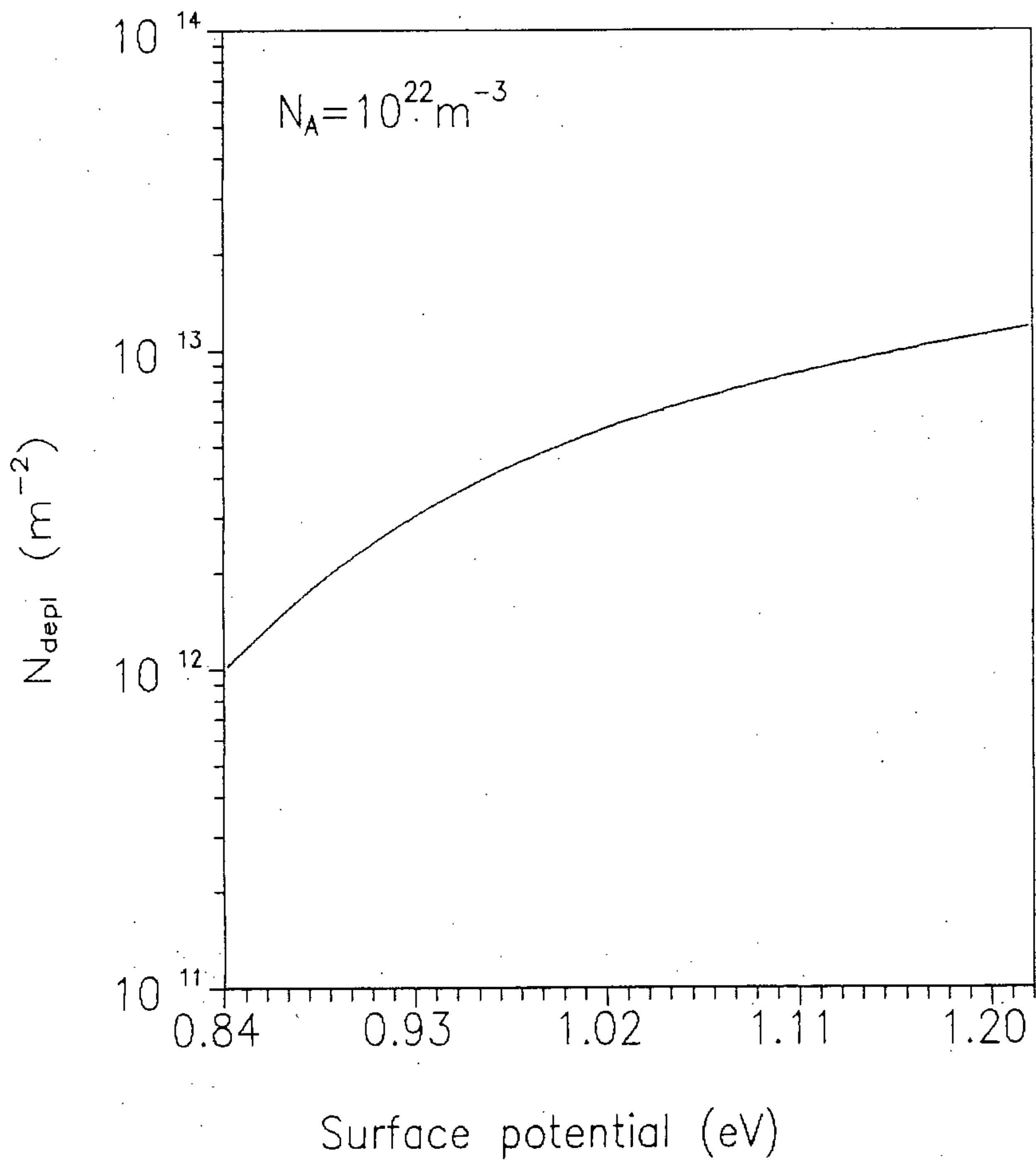

Fig. 3.4 Effect of surface potential on depletion charges.

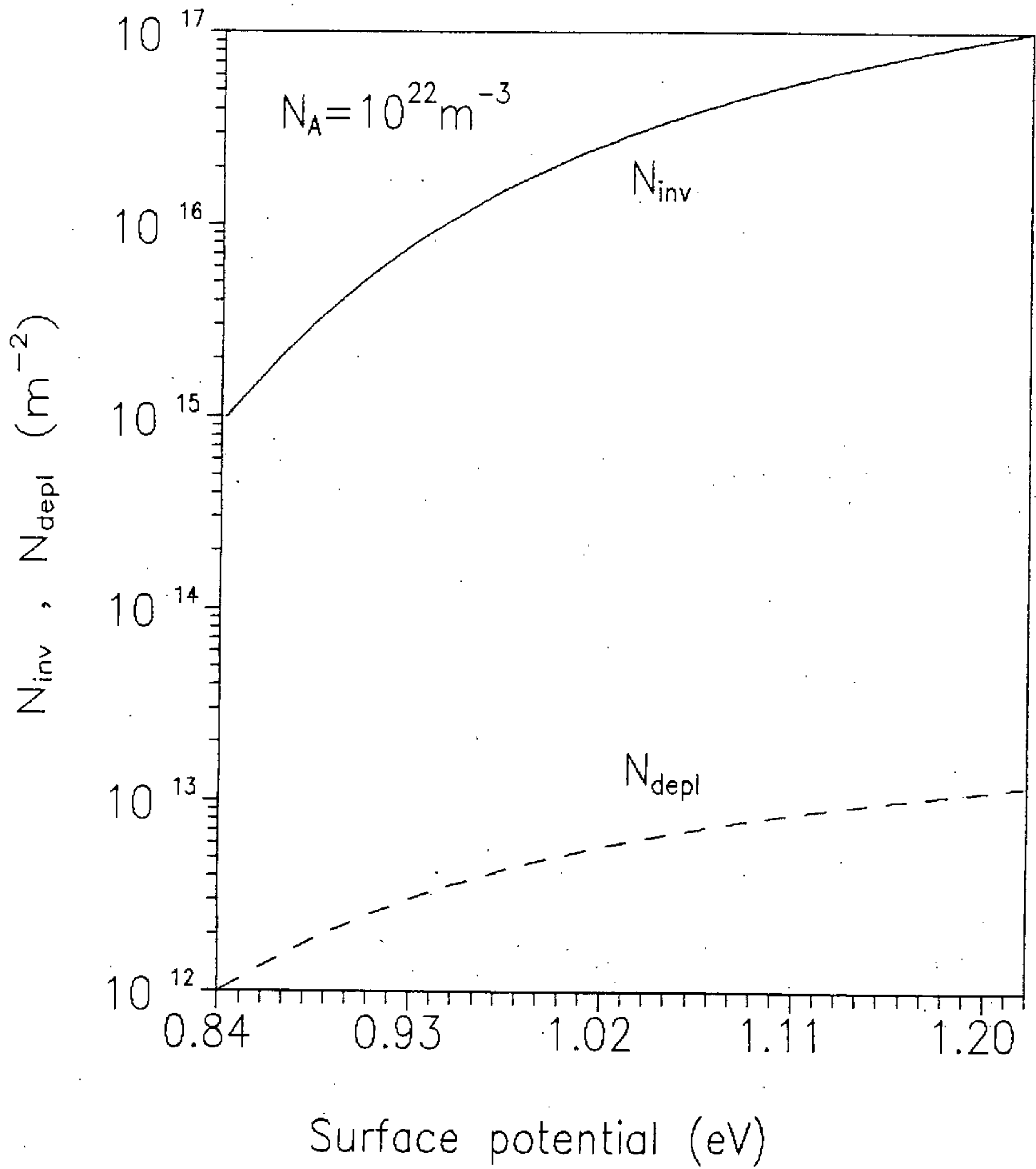

Fig. 3.5 Inversion and depletion charges vs. surface potential.

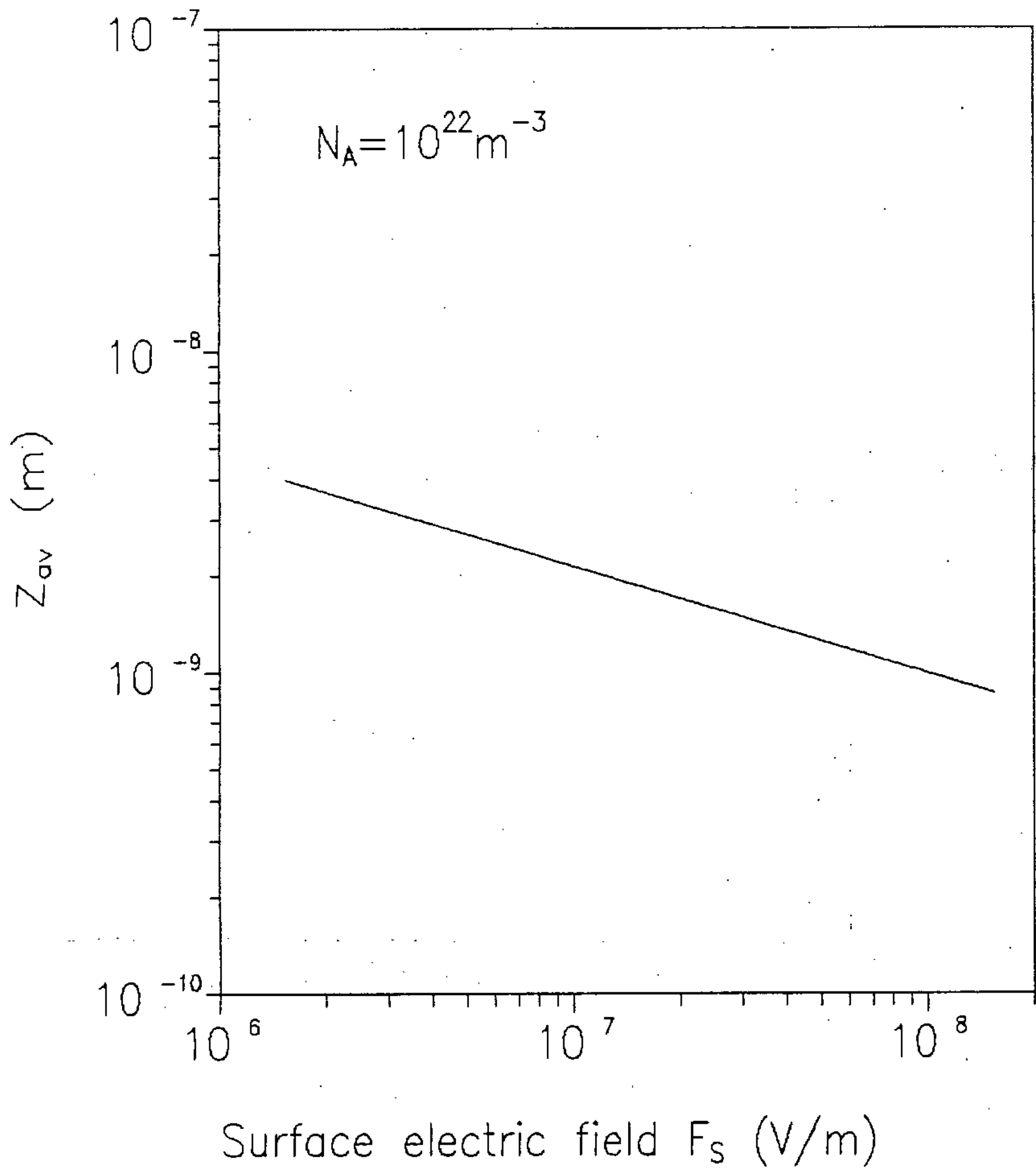

Fig. 3.6 Effect of surface electric field on average penetration of inversion charges from the Si/SiO_2 interface.

the inversion layer carriers from the Si/SiO_2 interface decreases with increasing surface electric field. As the gate voltage is increased the band bending at the Si/SiO_2 interface is increased. The width of the quantum potential well, therefore, is decreased and at the same time inversion layer carriers are more strongly attracted to the Si/SiO_2 interface. As a result the average penetration of the inversion layer charge carriers from the surface is decreased with increasing gate voltage.

3.3.5 Threshold voltage shift

The predicted threshold voltage shift, due to quantization, for devices with gate oxide thickness 10 nm is shown as a function of channel doping levels in (Fig.3.7). It is readily observed that the predicted threshold voltage shift, when the quantization effects in the inversion layer are included and when the classical prediction, i.e. no quantum effects are taken into account, increases markedly with increasing channel doping levels. It is important to account for this change in threshold voltage because of its strong role on the electrical characteristics, such as the drive current which directly influences the device speed.

For a given oxide layer thickness, as the channel doping level is increased the electric field perpendicular to the Si/SiO_2 interface becomes stronger and the quantum nature of the potential well becomes increasingly prominent. The band bending at the Si/SiO_2 interface becomes steep and the difference in the energy between the bottom of the conduction bend E_c and the first

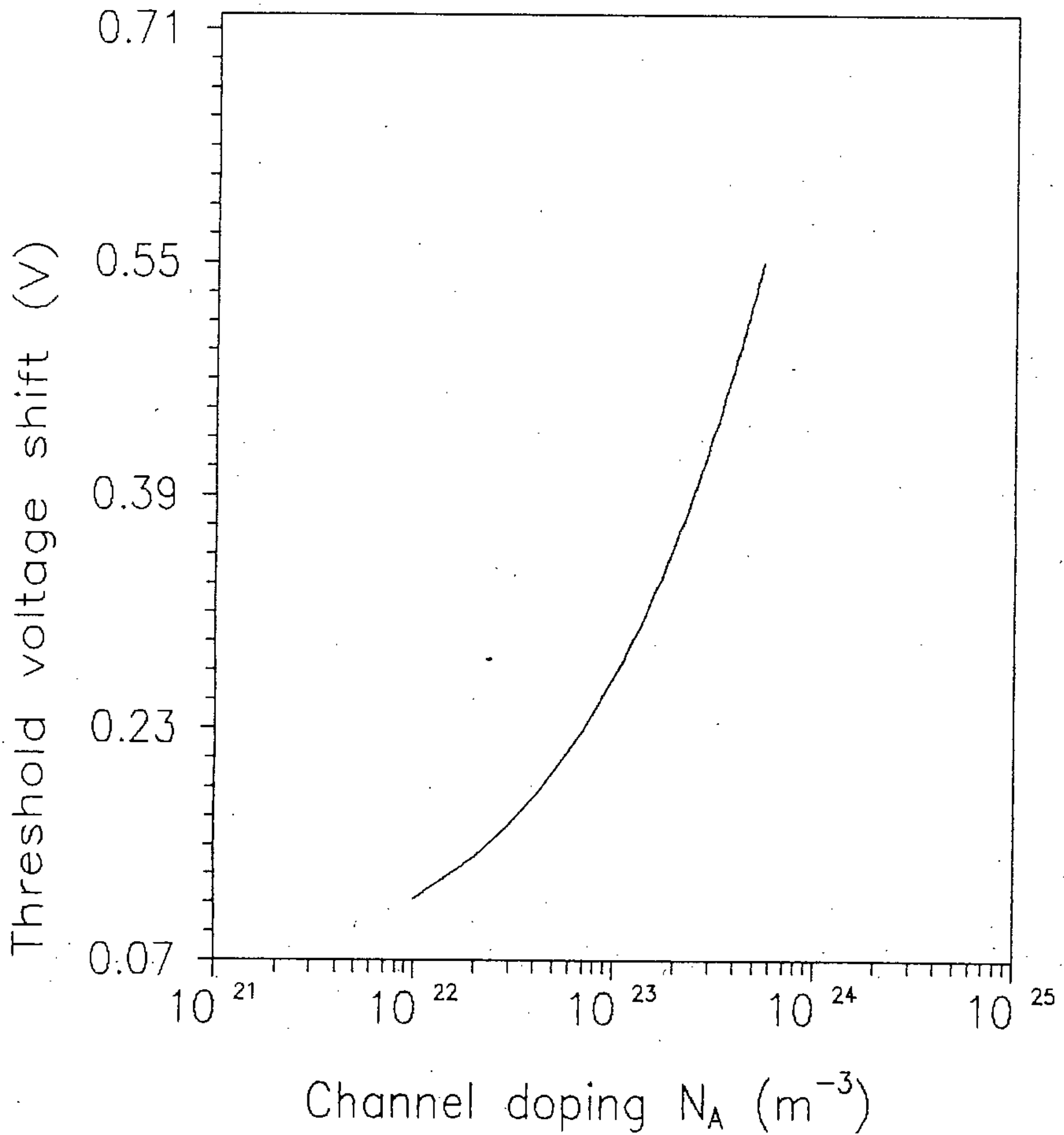

Fig. 3.7 Effect of channel doping on the difference between quantum and classical threshold voltage

allowed energy level E_0 increases. As a result to induce the same amount of inversion layer charges the threshold voltage must be increased. Again, the average separation of inversion layer carriers from the Si/SiO_2 interface is increased compared to the classical solution and, therefore, the voltage drop given by this increase of the average distance from the Si/SiO_2 interface times the normal electric field must be supplied by the gate voltage. Hence, the threshold voltage is also increased by this phenomena.

3.4 Summary

The mathematical model developed in chapter two is used here to determine the threshold voltage and other characteristics of the MOS device to study the quantum-mechanical effects on the inversion layer minority carriers.

In the triangular potential well the energy level is quantized and the lowest allowed energy level is shifted substantially above the bottom of the conduction band at the Si/SiO_2 interface. The shift is increased with increased gate voltage which increase the surface electric field. This is due to the fact that at increased surface electric field the band bending increases with the effect of producing steeper and deeper potential well. As a result the quantum-mechanical effects become more prominent and the lowest allowed energy level is correspondingly shifted above the bottom of the conduction band. Consequently the lowest allowed energy level can be used as a parameter to model the effect of the inversion layer quantization on the inversion charge density of the MOS devices.

Inversion layer charge concentration increases at a lower rate with increased gate voltage i.e. surface electric field when the quantum effects are considered. This is due to the fact that with the upward shift of the lowest allowed energy level the number of inversion layer carriers cannot increase at the previous rate which is exponential in nature.

The variation of depletion layer carriers is small compared to the inversion layer carriers. Contrary to the classical case where the depletion layer carriers become almost constant after the threshold voltage is reached (additional surface potential increases only the inversion layer carriers), the depletion layer carriers is found to be varying here. This is because the depletion layer width i.e. depletion layer carrier concentration is dependent more strongly on the inversion layer carrier concentration and their average penetration from the Si/SiO_2 interface.

Threshold voltage is the critical voltage at which the inversion layer is formed to a significant extent, giving rise to a rapid increase of the inversion layer charge for higher gate voltages. Physically the threshold voltage supports a bulk charge and at the same time introduces a band bending at the surface to reach the strong inversion potential. Quantum-mechanical effects shift the lowest allowed energy level and at the same time displaces the inversion layer carriers from the Si/SiO_2 interface. As a result increased gate voltage is needed to induce the same amount of inversion layer carriers. This increases the threshold voltage. With the increasing channel doping levels the normal electric field at the Si/SiO_2 interface is increased and

the increased effects of quantization results in a higher threshold voltage. Also the oxide layer voltage drop is dependent on the normal electric field. For a given channel doping level threshold voltage decreases with decreasing oxide layer thickness since the oxide layer voltage drop is less and a smaller gate voltage is needed to induce the same amount of inversion layer carriers.

CHAPTER 4

CONCLUSIONS

4.1 Conclusions

In this work an analysis is presented to study the quantum-mechanical effects in the inversion layer of low dimensional MOSFETs. The self-consistent solution of the Schrödinger and Poisson equations for the eigen energy of inversion layer potential well is very time consuming. In this work the potential well in the inversion layer is assumed to be triangular in shape and an analytical expression for eigen energy has been determined by solving Schrödinger wave equation with the help of WKB approximate method. The spatial distribution of the inversion layer carriers has been taken into account by evaluating their average distance into the semiconductor from the semiconductor-insulator interface.

A computer efficient analytical model is developed to determine threshold voltage of MOSFETs incorporating quantum-mechanical effects. Classical definition of threshold voltage is

used here to find a condition for quantum threshold voltage. High substrate doping levels and very narrow gate oxide thicknesses were used to investigate different MOSFET characteristics, under strong inversion conditions taking quantum-mechanical effects into account and the results are given. The model developed uses less CPU time and the results reflect the quantum-mechanical predictions. The difference between the quantum and classical threshold voltage is found to be strongly dependent on substrate doping level.

4.2 Suggestions for future work

The analytical model developed in this thesis describes the MOS characteristics in the electric quantum limit i.e., we have considered here only the lowest energy subband in the inversion layer potential well. It is possible in future to develop similar model by considering more energy subbands. Also Schrödinger wave equation could be solved using a variational method for a better approximate solution of the eigen energy.

REFERENCES

[1] B.G. Streetman, "Solid State Electronic Devices," Prentice Hall, New York, 1990, pp. 301-308.

[2] E.S. Yang, "Microelectronic Devices," Mc-Graw-Hill Book Company, New York, 1988, pp. 229-236.

[3] S.M.Sze, "Physics of Semiconductor Devices," John Willey, 1981, Chap 8.

[4] Frank Stern and W.E.Howard, "Properties of semiconductor surface inversion layers in the electron quantum limit," Physical Review, Vol.163, No.3, 1967, pp.816-835.

[5] Y. Ohkura, "Quantum effects in Si n-MOS inversion layer at high substrate concentration," Solid State Electronics, Vol.33, No.12, 1990, pp.1581-1585.

[6] Leonard I.Schiff, "Quantum mechanics," Mc-Graw Hill, New York, 1968, pp.268-279.

[7] J.A.Pals, "A general solution of the quantization in a semiconducyor surface inversion layer in the electric quantum limit," Physics letters,Vol.39A, 1972, pp.101-102.

[8] F. Stern, "Self-consistent results for n-type Si inversion layers," Physical Review B, Vol.5, No.12, 1972, pp.4891-4899.